PHYSICAL REVIEW A VOLUME 2, NUMBER 2 AUGUST 1970

Measurements of Absolute Cross Sections for (e, H_2) Collision Processes. Formation and Decay of H_2^- Resonances

A. Weingartshofer,* H. Ehrhardt, V. Hermann, and F. Linder

Institut für Physik der Universität Mainz, Mainz, Germany

(Received 22 December 1969)

Energy and angular dependences of the elastic and inelastic scattering of electrons from H_2 have been measured in the energy range 10 to 16 eV and for scattering angles ranging from 10° to 120°. Three resonance series have been investigated starting at 11.30, 11.50, and 13.63 eV, respectively. The last two series decay preferentially into one single electronic channel, while the first resonance (resonance I) decays into all energetically possible exit channels, i.e., $X\,{}^1\Sigma_g^+$, $b\,{}^3\Sigma_u^+$, $B\,{}^1\Sigma_u^+$. Throughout, stress is laid on the importance of absolute cross sections and reported values, and excitation functions have been presented in absolute units. The cross sections for the elastic channel and some inelastic channels ($X\,{}^1\Sigma_u^+$, $v=1$ and 2, and the dissociative continuum $b\,{}^3\Sigma_u^+$) are composed of resonant and nonresonant scattering and show pronounced and rapidly changing interference structures. Relative branching ratios for resonance series I in terms of absolute total cross sections have been listed for those channels where practically no direct scattering amplitude is present. Summarizing those results, one can state that the probabilities (branching ratios) for the decay of resonance series I into the three electronic states $X\,{}^1\Sigma_g^+$, $b\,{}^3\Sigma_u^+$, and $B\,{}^1\Sigma_u^+$ of the H_2 molecule summed over all vibrational states of the exit channel are of the same order of magnitude. From the observed angular dependence of the scattered electrons, the configuration of the resonances has been determined and compared with existing theoretical predictions.

INTRODUCTION

H_2 is the simplest molecule and therefore attractive for theoretical investigations. Similarly, the simplest molecular negative-ion system is the H_2^- which is responsible for a large number of resonances in the e-H_2 scattering. It can be hoped that quite reliable calculations, not only for energy positions[1,2] but also for cross sections of formation and probabilities of decay of such resonance states into different exit channels, can be carried out. Therefore it seems essential to provide as much detailed and quantitative experimental information as possible. Only little is known with respect to transition probabilities. The e-H_2 system is an interesting example in this respect as it possesses two very distinct types of resonance series; one that decays preferentially into one single electronic exit channel, while the other type branches out into all energetically possible exit channels. Examples of these two groups are the resonances that start at 11.30 and 13.63 eV, respectively. The region 11 to 13 eV deserves special attention since various authors[2,3] have suggested the possibility of other H_2^- states lying in this range.

In this paper an attempt has been made to follow through quantitatively the details of formation and decay into different exit channels of these compound states. From the observed angular dependence of the scattered electrons, their configuration has been determined and compared with existing theoretical predictions.[2]

We shall first review in general the present state of knowledge of the H_2^- states and give a survey of existing experiments on the scattering of low-energy electrons by H_2 and their theoretical analysis. Some of our results, to be discussed fully in subsequent sections, have been anticipated in this Introduction to clarify certain concepts.

Figure 1 illustrates the potential energy curves of some H_2^- states and also some electronic states of the hydrogen molecule which are relevant to this discussion. The limits to which these states tend as the nuclear separation tends to infinity have been drawn for the lower state $[H(1s)+H^-(1s^2)]$ and have been omitted for higher states, since several dissociation asymptotes may exist, e.g.,

$$H_2^{-*} \to H(nl) + H^-(1s^2) \to H^-(nl, n'l') + H(1s), \quad \text{etc.}$$

The ${}^2\Sigma_u^+$ resonance in the 3-eV region is well documented.[4,5] The ${}^2\Sigma_g^+$ resonance at 10 eV is of interest because of its role in dissociative attachment in e-H_2 collisions and in electron-associative detachment in H-H⁻ collisions.[6] The resonance at 14 eV has been reported recently by Ehrhardt and Weingartshofer.[7] Values of the vibrational levels are as follows (in eV):

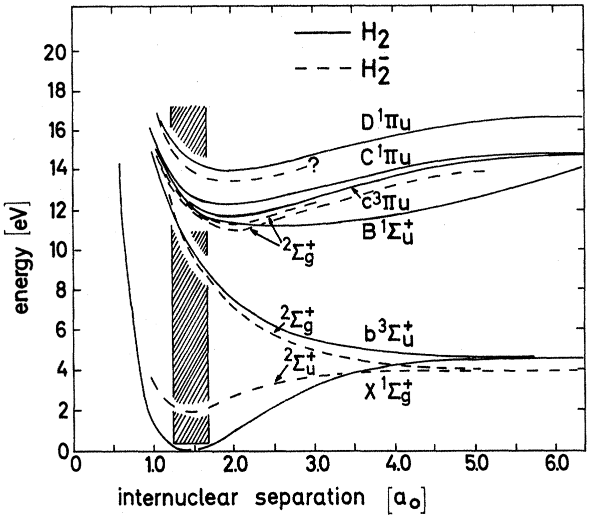

FIG. 1. Potential energy curves for some H_2^- resonances (dashed lines, see text and Ref. 2) and some H_2 states (full lines). The shaded area represents the Franck-Condon region for excitation from the ground vibrational and electronic state of H_2.

H_2^-	$v=0$	$v=1$	$v=2$
	13.63	13.93	14.20
	$v=3$	$v=4$	$v=5$
	14.47	14.70	14.92 .

The resonance shows the peculiar characteristic that it decays preferentially into the $C\,^1\Pi_u(v=0, 1, 2, \ldots)$ vibrational states of H_2. Since the observed transitions of significant intensity occur between identical vibrational quantum numbers of the H_2^- and $C\,^1\Pi_u$ states it is very likely that the potential energy curves of the new H_2^- state should have the same shape and internuclear distance as the $C\,^1\Pi_u$ – as well as the $D\,^1\Pi_u$ – state of H_2. Therefore it is assumed that the core of the negative-ion state has a $^1\Pi_u$ configuration and angular dependences of the resonance indicate that the over-all configuration of the H_2^- is $^2\Sigma_g$. The nuclear separation of the core does not change significantly during the autoionization process. The corresponding potential energy curve has been drawn simply by shifting the potential energy curve of the $C\,^1\Pi_u$ state of H_2 to the measured energy position.

The scattering of electrons in the energy range 11 to 13 eV by H_2 and its isotopes has been investigated by several groups.[3,8-10] This region is interesting because the elastic and inelastic cross section show a lot of structure. Kuyatt, Simpson, and Mielczarek[3] have tabulated the resonance energies of the transmission peaks and ascribed this structure to the vibrational levels of two resonances. The surprising feature of these results is that pairs of resonances are nearly equal in size for HD, while H_2 and D_2 show predominantly only one strong series of resonances with an indication of a weaker series, but the over-all pattern is similar to that of HD. Because of their appearance in H_2 (strong peaks and shoulders), these two series are sometimes referred to as the "strong" and "weak" series. Transmission experiments give information on the formation of the compound state; therefore, the expressions strong and weak may be used only in this sense. In differential cross-section measurements both formation and decay are determining factors for the observed intensities in a given channel. Therefore, depending on the experiment, a weak resonance may very well appear stronger than a strong resonance in the above sense. Because of this we will be using the nomenclature resonance I and II instead of strong and weak series. The configuration of resonances I and II could not be determined in the measurements of Kuyatt *et al.*, nor did the authors consider the possibility that some of the structure might arise from interference effects between the potential and resonant scattering. The calculation of energy and vibrational structure of these resonances was initiated by Taylor and Williams[1] and greatly improved by Eliezer, Taylor, and Williams.[2] These authors predicted a total of four resonances in the 11–13-eV energy range, two of which were identified with the resonance series I and II. They proposed the configuration $^2\Sigma_g^+$ for both. The outstanding result of these calculations is that resonance I is represented by an electron bound to the $c\,^3\Pi_u$ state of H_2, while resonance II represents almost purely the electron bound to the $C\,^1\Pi_u$ state. Heideman, Kuyatt, and Chamberlain[9] observed the energy dependence of the excitation cross sections of the $v=0$ and $v=1$ vibrational states of the $B\,^1\Sigma_u^+$ state of H_2. In both curves, several sharp resonances occur, which these authors clearly relate to the resonances in the total scattering cross-section measurements by Kuyatt *et al.*[3] In the same laboratory Menendez and Holt[10] observed resonance structure in the electron scattering from H_2 in the forward direction in two inelastic channels $v=1$ and $v=2$ of the electronic ground state of H_2. These authors felt that it was impossible to state conclusively on the basis of their work, whether the two H_2^- series proposed by Kuyatt *et al.*[3] could fully account for the resonance structure in the inelastic channels. They noticed that the resonance shapes in the inelastic channels differ from those in the transmission (elastic) channel and from one another.

In this work we try to trace out a picture as complete as possible of the e-H_2 resonance system in the 11–15-eV region. In particular, we attempt to relate the different resonance structures to resonance states (series) and also to determine the configurations of the resonances and branching ratios for their decay into various exit channels. We have measured differential excitation functions (energy dependences of the intensity of the scattered electrons into a given decay channel for a fixed scattering angle) and angular dependences of the intensity of the scattered electrons for fixed primary energy and a given decay channel. The following exit channels have been investigated: (a) the $B\ ^1\Sigma_u^+$ state in the vibrational states $v = 0, 1, 2, 3$; (b) the $b\ ^3\Sigma_u^+$ dissociative continuum for small energy windows around 10.17, 10.47, 10.76, 11.02 eV, and other energy values, (c) the electronic ground state of H_2: $X\ ^1\Sigma_g^+$, $v = 0, 1, 2, 3, 4, 5$; (d) the two triplet states of $a\ ^3\Sigma_g^+$ and $c\ ^3\Pi_u$; (e) the $C\ ^1\Pi_u$ state in the vibrational states $v = 0, 1, 2, 3$; (f) two channels, which were not resolved and consist mainly of $C\ ^1\Pi_u$ ($v = 4, 5$) and probably admixtures of $B'\ ^1\Sigma_u^+$ and $D\ ^1\Pi_u$ states. In the section on experimental results we deal mainly with points (a)-(d) while most of the results contained in (e) and (f) have already been reported in a previous paper.[7]

EXPERIMENTAL PROCEDURES

The experimental arrangement consists of a monochromatic electron beam of ~10^{-8} A and a full width at half-maximum between 30 and 80 meV. The incident beam of which the energy can be varied between 8 and 30 eV is crossed at right angles with a molecular beam (~10^{-3} Torr). The scattered electrons are energy selected in a second 127° electrostatic analyzer and detected with a 17-stage multiplier. The collector system can be rotated from 0° to 120°.

The scattered electrons are counted and the signal can be plotted analog on an X-Y recorder or the counting rate can be stored over the period of several hours in a multichannel scaler. The output is plotted on an X-Y recorder through a digital-to-analog converter. The apparatus, as well as the technique of modulation to free the signal from background contributions, has been discussed in a previous paper.[5,11]

We employed two methods to calibrate the energy scale: (i) observation of the onset energy of known inelastic processes in H_2; (ii) direct comparison with the 19.31-eV resonance in He using a H_2-He gas mixture and observing the elastic scattering at an angle of 100°, where the resonance series in H_2, as well as the He resonance appears as a uniform destructive pattern (see Fig. 5). The two methods agree within 20 meV.

The following procedure was adoped to calibrate our measurements on an absolute scale. The ratios of the measured inelastic intensities to the elastic differential cross sections were obtained directly from energy-loss spectra. Special care was taken to ensure an energy-independent transmission of the electron optical systems.[5,11] The experimental uncertainty in this respect should not exceed 10-15% over an energy range of about 10 eV. Absolute e-H_2 scattering cross sections from other experiments[12,13] have been used to put all measured intensities, inelastic as well as elastic cross sections, on an absolute scale. The over-all error in determining the absolute values is of the order of 20%.

EXPERIMENTAL RESULTS

Exit Channel $B\ ^1\Sigma_u^+$ ($v = 0, 1, 2, 3$)

Figure 2 shows the energy dependence of the absolute differential cross section of the three lowest vibrational levels in this electronic state. The curves were smoothed to bring out the more prominent resonance peaks which can be measured with an absolute reproducibility of ±0.02 eV in all our tracings. The curves for $v = 0$ and $v = 1$ are very similar to the excitation functions published by

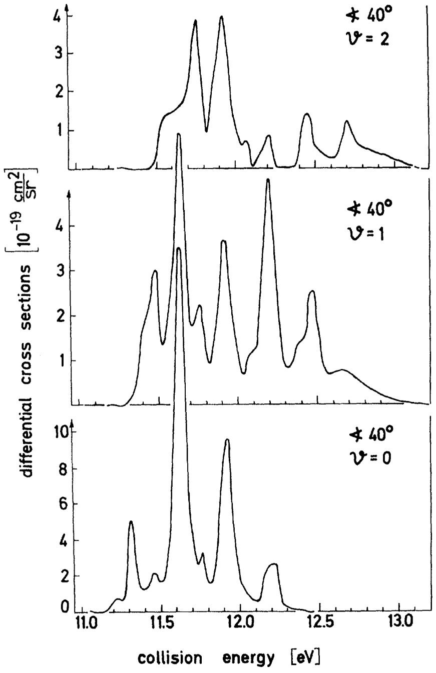

FIG. 2. Energy dependence of the absolute differential cross sections for excitation of the $v = 0, 1$, and 2 vibrational levels of the $B\,^1\Sigma_u^+$ state of H_2. The scattering angle is 40° and the curves were smoothed to bring out the significant structure that appears in all tracings. Note the different absolute scales. Resonance series II appears weak in the channel $v = 0$, but rather strong in the channels $v = 1$ and 2.

Heidemann *et al.*[9] However, it should be remarked that our curves do not suffer from nonphysical background contributions and from them it can be clearly seen that the direct nonresonant scattering amplitude is remarkably small, but increases very much at higher collision energies (not shown in the figure). Also note that the cross sections in Fig. 2 are given in absolute units.

These resonance peaks can be grouped into two series which decay into the $H_2\ B\ ^1\Sigma_u^+$ ($v=0, 1, 2$) channels with a rather large probability. The resonance energies are listed in Table I. For comparison the measured values of Kuyatt *et al.*[3] and the calculated values of Eliezer *et al.*[2] are given also.

Two things are to be noticed. For the series I, our values deviate systematically from the values of Kuyatt *et al.*[3]; however, they agree with the calculated values. For the series II, there is a moderate agreement of all measured values (ours included) with the calculated values in Table I. The discrepancy between the data of Kuyatt *et al.*[3] and this work can be explained by the different method of determination of the resonance energies. The numbers of Kuyatt *et al.*[3] are derived from peak positions in the transmitted current. These peak positions need not be the true energy positions of the negative-ion states, since strong interference effects between resonant and nonresonant scattering probably cause more complicated resonance structures than just simple peaks. On the other hand, simple resonance peaks (because of the absence of direct scattering contributions) have been used for energy level determination in our work.

The total cross section, which is measured in a transmission experiment, is mostly determined by the elastic scattering. Our elastic cross-section data (see Fig. 5) can be explained as a result of interference structure caused only by resonance I (without observable contributions from resonance II). It would be worthwhile to carry out an investigation to see if the structure in the transmission experiment could not also be explained by taking into account resonance I only, and if the observed shoulders could be reproduced by interference effects. If one assumes the shape parameter $q=-1$ for the resonances measured by Menendez and Holt[10] in transmission and takes the points of steepest descent to be the true energy positions of the resonances, then good agreement with the energy positions of our work can be obtained. In a model with narrow neighboring resonances with shape parameters $q=\pm 1$, the direct-scattering contribution produces a shoulder between two consecutive resonances. However, only a partial-wave analysis will be able to clear up this question.

TABLE I. Energy positions (in eV) of resonance series I and II.

This paper[a]		Calculated[b]		Kuyatt *et al.*[c]	
I	II	I	II	I	II
		11.07			
11.30		11.37		11.28	
	11.50		11.46		11.46
11.62		11.66		11.56	
	11.79		11.75		11.72
11.92		11.93		11.84	
	12.08		12.03		11.99
12.20		12.19		12.11	
	12.38		12.31		12.27
12.46		12.43		12.37	
			12.58		12.53
12.70		12.65		12.62	
			12.84		12.77
				12.86	
			13.09		12.97

[a] Estimated error ±0.02 eV.
[b] Eliezer *et al.* (Ref. 2).
[c] Reference 3.

The configuration of the negative-ion states can be determined by angular dependence measurements of the scattered intensity. For resonance series I this is illustrated in Fig. 3 for two different decay channels $X\ ^1\Sigma_g^+$ and $B\ ^1\Sigma_u^+$. If a $^2\Sigma_g^+$ configuration for the negative-ion state is assumed, then the autoionization into the $X\ ^1\Sigma_g^+$ state of the molecule leads to a σ_g assignment of the outgoing electrons, i.e.,

$$H_2^-(^2\Sigma_g^+) \rightarrow H_2(X\ ^1\Sigma_g^+) + e^-(\sigma_g)\ . \tag{1}$$

In a first approximation[14-16] one has to expect an s-wave angular distribution for σ_g electrons. This is in accordance with the measurements of Fig. 3 (right-hand side). The exit channel $v=4$ has been chosen, since only in this channel is the pure autoionization process observed without direct-scattering contributions (see Fig. 7). In contrast to Eq. (1), the autoionization into the $B\ ^1\Sigma_u^+$ state of H_2 leads to a σ_u electron, i.e.,

$$H_2^-(^2\Sigma_g^+) \rightarrow H_2(B\ ^1\Sigma_u^+) + e^-(\sigma_u)\ . \tag{2}$$

In an expansion in l of a σ_u outgoing wave one expects a dominating p-wave ($p\sigma$) contribution. This has been measured (see Fig. 3, left-hand side) and found in agreement with the theoretically predicted $(1+2\cos^2\theta)$ angular dependence (full line).

In Table II the angular dependences of all prominent peaks (see Fig. 2) for the transitions into the $B\ ^1\Sigma_u^+$ ($v=0, 1, 2$) states are listed. All the peaks belonging to series I have a clear p-wave character. In addition, a systematic energy dependence of the angular distributions is observed,

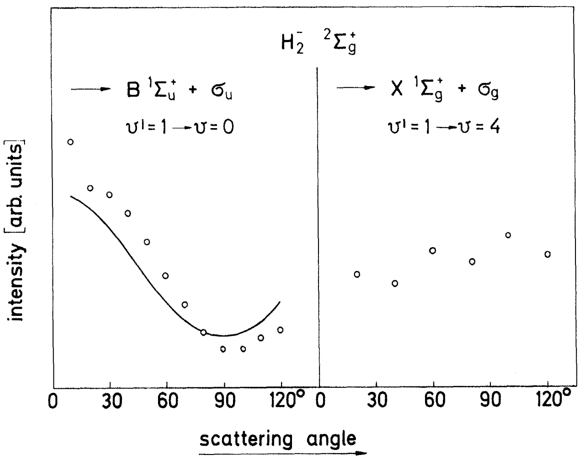

FIG. 3. Angular dependence of the scattered electrons for the decay of resonance series I into two different electronic channels. The full line (left figure) represents the simplest theoretical prediction (Refs. 14-16) for the angular dependence of σ_u electrons. The simplest prediction for σ_g electrons gives an isotropic angular distribution (right figure).

i.e., the angular dependences are steeper for higher kinetic energies of the outgoing electrons. A change with energy is to be expected[16] since the higher partial waves in the l expansion of the autoionizing electrons become more important with increasing kinetic energy. (The small relative variations of the energy of the colliding primary electrons cannot affect the angular dependences.)

Table II gives angular dependences of only the two most prominent peaks of series II. Unfortunately, these peaks have an unsymmetrical shape and do not lend themselves to a clear interpretation. In addition, the experimental errors incurred in the measurements on small peaks of series II are rather large. However, although conclusions are not definite, one can say that our results do not contradict the possible configuration ${}^2\Sigma_g^+$ for series II as has been predicted.[2]

Before discussing the other exit channels we would like to make two general remarks about resonance series I and II. First, series I has the peculiar characteristic of decaying with a fairly large probability into all energetically possible electronic exit channels ($B\,{}^1\Sigma_u^+$, the dissociative continuum $b\,{}^3\Sigma_u^+$, and the electronic ground state $X\,{}^1\Sigma_g^+$). In contrast, series II decays with a large probability only into the vibrational levels $v = 1$ and 2 of the $B\,{}^1\Sigma_u^+$ electronic state.

Secondly, we would like to remark that we have looked carefully for the predicted[2] first level at 11.07 eV of series I, but could not observe it in any of the exit channels. It has been suggested that the reason for this could be a very small Franck-Condon factor for the formation of the compound state from the molecular ground state. On the other hand, experiment (Fig. 1 of Ref. 7) gives rather large Franck-Condon factors for the $v = 0 \rightarrow 0$ transitions from the ground state $X\,{}^1\Sigma_g^+$ into the two excited states $c\,{}^3\Pi_u$ and $C\,{}^1\Pi_u$ of H_2. Since the potential curves of the two resonances are predicted[2] to be similar in shape and internuclear distance, it is difficult to see why the Franck-Condon factors should be so different in the case of formation of the negative ions. We have, therefore, referred in this work to the first observed levels of both series I (11.30 eV) and II (11.50 eV) as $v = 0$.

McGowan and Williams have recently reported[17] the resonance excitation of the $B\,{}^1\Sigma_u^+$ state by measuring the vacuum ultraviolet radiation which re-

TABLE II. Absolute differential cross sections in 10^{-19} cm^2 for the decay into exit channel $B\,{}^1\Sigma_u^+$ ($v = 0, 1, 2$) of resonance series (rs) I and II.

	rs I (v')								rs II (v'')	
Scattering angle (deg)	$v' = 0$ $v = 0$	$v' = 1$ $v = 0$	$v' = 2$ $v = 0$	$v' = 1$ $v = 1$	$v' = 2$ $v = 1$	$v' = 3$ $v = 1$	$v' = 2$ $v = 2$	$v' = 4$ $v = 2$	$v'' = 0$ $v = 1$	$v'' = 1$ $v = 2$
10	9.9	27.4	16.0	8.5	6.4	6.5	5.2	2.1	6.0	4.8
20	7.4	22.5	13.4	6.2	4.9	5.8	4.2	1.8	4.4	3.5
30	6.4	21.8	11.7	6.3	4.7	5.5	4.1	1.4	4.0	3.1
40	5.4	20.0	9.5	6.0	3.6	5.0	4.0	1.1	3.0	3.3
50	5.1	17.0	7.6	5.4	3.0	4.5	3.8	1.0	2.7	3.3
60	4.9	13.5	5.7	4.8	2.3	3.8	4.3	1.0	2.4	3.2
70	4.4	10.5	3.7	3.8	2.1	3.0	3.7	1.1	2.5	2.9
80	4.2	7.9	2.9	2.8	1.5	2.2	3.2	1.0	2.0	2.7
90	4.1	6.0	2.3	2.3	1.6	1.9	2.8	0.9	1.7	2.5
100	4.2	6.0	2.3	2.1	1.4	1.9	2.3	0.9	1.8	2.4
110	4.4	7.1	2.9	2.0	1.8	2.3	2.0	0.9	1.7	2.2
120	5.0	7.9	3.1	2.5	2.1	2.5	2.1	0.7	2.0	1.8

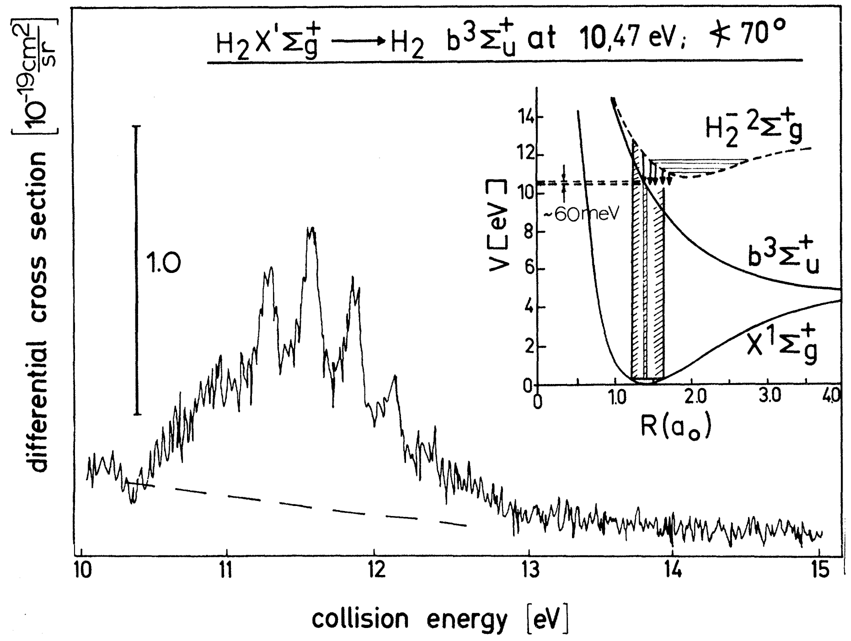

FIG. 4. Energy dependence of the absolute differential cross section for excitation into a narrow band (~60 meV) at 14.47 of the dissociative continuum $b\,^3\Sigma_u^+$ channel by electron collision with H_2. The zero line is dashed. The length of the bar to the left of the curve represents the absolute scaling factor in units of 1.0×10^{-19} cm^2/sr. The insert illustrates the autoionization of the H_2^- ion into the energy band. The Franck-Condon region is subdivided: The direct excitation can only occur in the center part, while transitions into the resonance take place over the whole width.

sults from the (e, H_2) collisions. There is qualitative agreement between our data and this work; however, the results of these authors lie some 90 meV above ours along the energy scale.

Exit Channel $b\,^3\Sigma_u^+$ (Dissociative Continuum)

Figure 4 shows the excitation function of the $b\,^3\Sigma_u^+$ state. Since in the experiment electrons are detected which have lost 10.47 eV, only transitions into a narrow band (~60 meV width) of the $b\,^3\Sigma_u^+$ potential energy curve are observed. This is represented in the insert of Fig. 4. To within 0.03 eV the resonance peaks occur at the same energies as in series I. The broad maximum represents the nonresonant contribution of the $b\,^3\Sigma_u^+$ excitation which has a maximum near 11.5 eV and decreases with increasing collision energy. The direct excitation into this state has been investigated at higher collision energies by Trajmar *et al.*[18] The probability for the transition $H_2^-(^2\Sigma_g^+)\rightarrow H_2(b\,^3\Sigma_u^+)$ is large for small energy differences but decreases continuously with increasing energy difference. The probability becomes negligible for the decay to a point on the potential energy curve of the $b\,^3\Sigma_u^+$ state outside the Franck-Condon region, although this region would be accessible because the lifetime of the H_2^- ion is sufficiently long for molecular vibrations.

Exit Channel $X\,^1\Sigma_g^+$ ($\nu = 0, 1, 2, 3, 4, 5$)

Figure 5 shows the energy dependence of the absolute differential elastic cross section for different scattering angles. Again the resonance

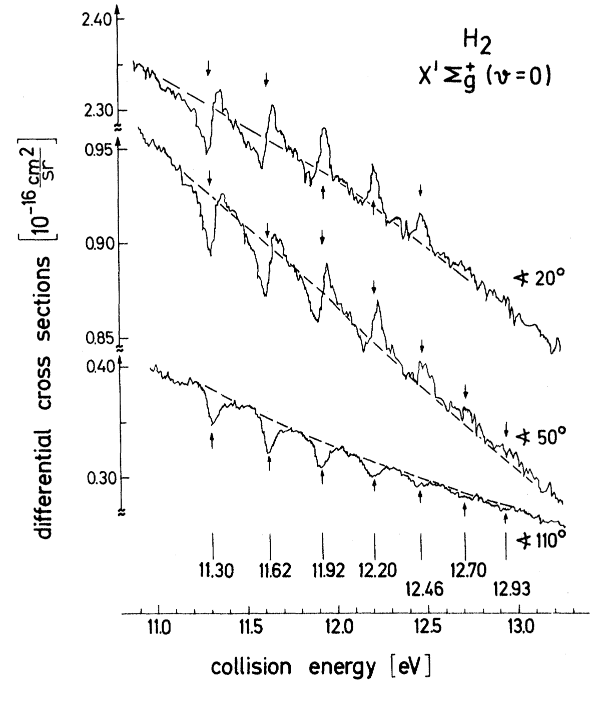

FIG. 5. Energy dependence of the absolute differential cross sections of the electronic and vibrational ground state of H_2 (elastic channel) for three different scattering angles. Note the different absolute scales to the left. The dotted lines were constructed by extrapolation of the low- and high-energy sides of the direct elastic scattering and have been traced in to bring out the rapid variation of the shapes of the resonance peaks with collision energy and scattering angle. The energy positions of the resonance peaks (see text for calibration) are shown at the bottom and are indicated with vertical arrows for each curve.

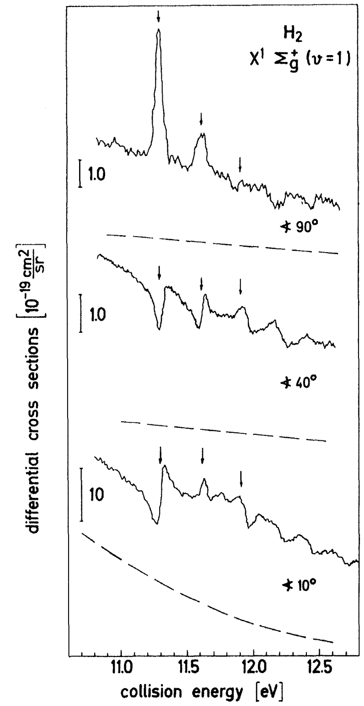

FIG. 6. Energy dependence of the absolute differential cross sections of the $v = 1$ vibrational level of the electronic ground state of H_2 for three different scattering angles. The zero lines are dashed. The length of the bars to the left represent the scaling factors in units of 10.0×10^{-19} cm^2/sr. for the 10° curve and 1.0×10^{-19} cm^2/sr. for the 40° and 90° curves. Note the rapid change of peak shapes with collision energy and scattering angle.

structure is caused by resonance series I and energy positions shown at the bottom of this figure were obtained by direct comparison with the 19.31-eV resonance in He using a H_2-He gas mixture and observing the elastic scattering at an angle of 100°, where the resonance series in H_2 as well as the He resonance appears as a uniform destructive pattern. These energy positions are indicated with vertical arrows on each curve to indicate the complexity of the interference patterns at small scattering angles. The dashed lines were also traced in for the same purpose and were constructed by extrapolation of the low- and high-energy sides of the curve for direct-elastic scattering. The rapid variation of the shapes of the resonance peaks with collision energy is almost spectacular. This phenomenon is unknown from resonance series in other molecules, e.g., N_2, CO, NO, CO_2, etc. It seems implausible to explain this phenomenon by the assumption that the phases for the potential scattering could change so rapidly, that by interference the shape of the resonances should vary in the observed manner. It should be noted that the collision energy is of the order of 11 to 13 eV and that we are considering elastic scattering, i.e., the potential phase would have to change by about 45° over an energy range of approximately 0.5 eV. It seems to us that further theoretical investigations are needed to account for this phenomenon. The peculiar variation of resonance shapes with collision energy can also be observed in the inelastic vibrational channels.

A selection of excitation functions for excitation of the vibrational levels $v = 1$, 2, 3, and 4 of the ground electronic state are presented in Figs. 6–8. The energy positions of the most prominent resonances are indicated by small vertical arrows. Within the limits of experimental accuracy, all resonance structure in these figures can be explained by resonance I, with the possible exception of the small feature close to 11.8 eV that can be seen on the 10° curve in Fig. 6 (see also curve *A* of Menendez and Holt[10]). The zero lines are dashed, and have been obtained from energy-loss spectra taken at different collision energies. Whereas the resonance contributions in different exit channels are of comparable magnitude, the amount of direct excitation of vibrational states decreases quite rapidly with increasing vibrational quantum num-

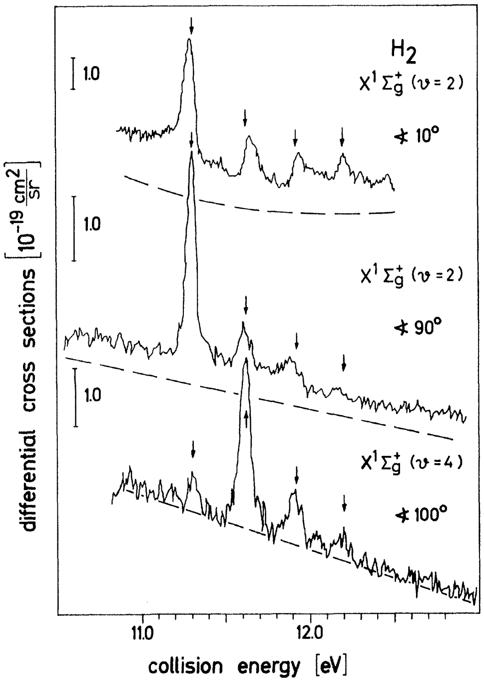

FIG. 7. Energy dependence of the absolute differential cross sections for different scattering angles and into two different exit channels, $v = 2$ and 4 of the electronic ground state. The zero lines are dashed. The length of the bars to the left represent the scaling factors in units of $1.0 \times 10^{-19} cm^2/sr$.

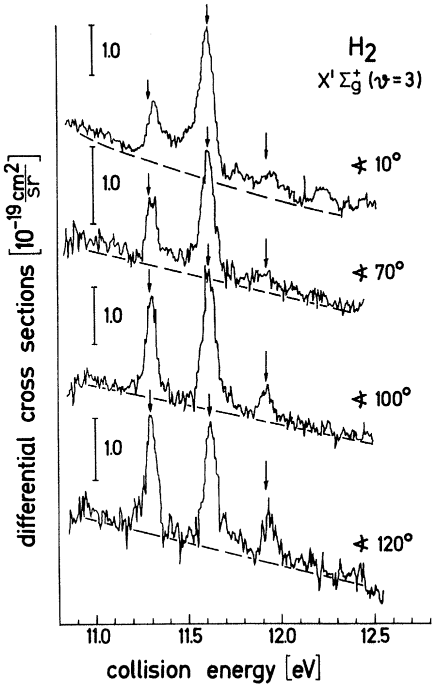

FIG. 8. Energy dependence of the absolute differential cross sections of the $v = 3$ vibrational level of the electronic ground state of H_2 for four different scattering angles. The zero lines are dashed. The length of the bars to the left of each curve represents the absolute scaling factors in units of 1.0×10^{-19} cm^2/sr.

bers. The angular dependences of the pure-resonant and pure-nonresonant vibrational excitation of the H_2 molecule in its electronic ground state are distinctly different. In contrast to the nearly constant angular distribution for the resonant excitation (see Fig. 6) the nonresonant part exhibits a pronounced minimum close to 70° scattering angle. Franck-Condon factors vary drastically with respect to the exit channel (see Fig. 7, $v = 2$ and 4) and are useful for construction of potential energy curves. A surprising finding is presented in Fig. 8. The three observable resonance peaks in the same exit channel show quite different angular dependence. This does not necessarily indicate a breakdown of the Born-Oppenheimer approximation. This could also be explained by interference between the resonance and the very small direct-scattering amplitude. Indications for this are the angular dependence of the shape of the resonances, the different size of the saddle between the first two peaks and the shift of the maximum of the first resonance with respect to the second one. Independent measurements of the resonance decay into the electronic ground state $v = 0$, 1, and 2 performed by Comer and Read[19] are in very good agreement with the present results. The direct-scattering contributions into these channels also agree very well with recent measurements by Trajmar *et al.*[20]

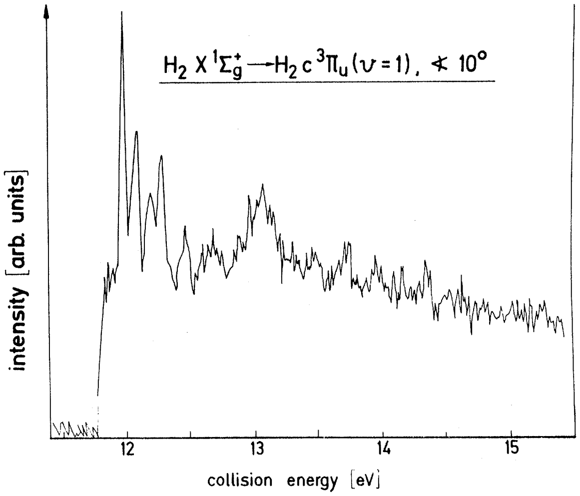

FIG. 9. Differential excitation function for the $c\,^3\Pi_u$, $v = 1$ vibrational level. Admixtures of the $a\,^3\Sigma_g^+$ state due to insufficient resolution should be small (Refs. 21, 22). No clear resonance series are discernible in the abundant resonance structure.

Other Exit Channels

In the course of this work, a number of other excitation functions have been measured, namely, the triplet states $c\,^3\Pi_u$, $a\,^3\Sigma_g^+$, and several vibrational states of the $C\,^1\Pi_u$, $B'\,^1\Sigma_u^+$, and $D\,^1\Pi_u$ channels. Some of these states could not be resolved. All

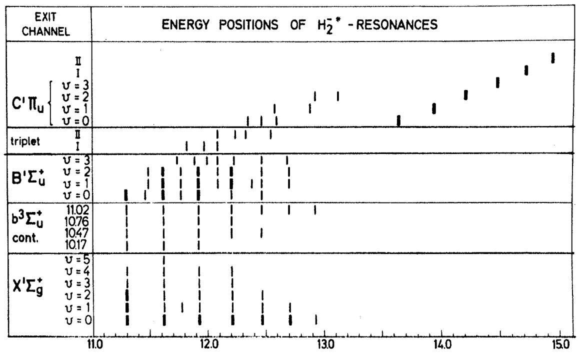

FIG. 10 Compilation of resonance lines observed in the indicated decay channels. The thickness of the lines is indicative of the measured transition strength. Triplets I and II stand for the unresolved states $c\,^3\Pi_u$ and $a\,^3\Sigma_g^+$ with predominant contribution from the c state (see Refs. 21 and 22). I and II in the top lines stand for $C^1\Pi_u$, $v = 4$ and 5 with some unresolved admixture of the $B'\,^1\Sigma_g^+$ and $D'\,^1\Pi_u$ states.

these measurements show lots of structure, especially close to threshold. Figure 9 gives an example. This structure is the result of interference of resonances with each other and with direct-scattering contributions. Therefore, it is very difficult at the moment to determine energy positions and configurations of possible resonances. In Fig. 10 only positions of some maxima for these channels are given, which do not necessarily coincide with true energy positions. All these measurements may be regarded as strong evidence for the existence of resonance states other than series I and II.

Recent measurements[22] with the trapped-electron method have also shown resonance structure in these channels.

SUMMARY

Figure 10 shows a compilation of the different resonance lines that have been found in this investigation. Given are the energy positions of the resonance states and the exit channels in which they were observed. Three clear resonance series appear; (i) resonance series I starting at 11.30 eV which decays into all energetically possible channels; (ii) four members of resonance series II starting at 11.50 eV which decays preferentially into the $B\,^1\Sigma_u^+$ channel; (iii) six members of a third resonance series starting at 13.63 which have been observed. This series decays almost exclusively into the $C\,^1\Pi_u$ channel, with predominant transitions occurring with the same vibration quantum numbers between the H_2^- ion and the $C\,^1\Pi_u$ state of the H_2. The exit channels above $B\,^1\Sigma_u^+$ $(v=2)$ show a lot of resonance (maxima, respectively, minima). It is very likely that some of this structure may arise from other negative-ion states.

An approximate half-width of resonance series I of 40 meV has been measured by direct comparison with the He resonance at 19.31 eV using a He-H_2 mixture and observing the elastic scattering at an angle of 100°. Objections can be raised that in such an experiment the resonance could be broadened by the presence of H_2^+ ions that would necessarily be formed. No broadening of the He resonance was observed. By the uncertainty principle the measured half-widths of the three resonances correspond to a lifetime of the order of 10^{-14} sec; therefore, decay of any of these resonances by light emission $(\tau \sim 10^{-9}$ sec) is highly improbable.

The outstanding behavior of resonance series I is that it decays into all energetically accessible exit channels. Table III gives absolute total cross sections for the decay of this resonance series for most of the exit channels where this series could clearly be identified. In order to give a complete picture for the decay of the resonance into the various exit channels it would be desirable to determine the branching ratios for all the processes. If I_i is the intensity of resonance scattering into channel i (integrated over all angles) and $\Sigma_i I_i$ is the sum of intensities over all decay channels, then the branching ratio for channel i is defined as the ratio of these two quantities. It is directly related to the partial width Γ_1 and total width $\Gamma = \Sigma_i \Gamma_i$ (see, for example, Ref. 23).

In the case of the $H_2^-\,^2\Sigma_g^+$ resonance (series I) the situation does not consist simply in taking the branching ratios from the experimentally determined intensities, because in several important exit channels $(X\,^1\Sigma_g^+,\ v=0, 1, 2)$ strong interference

TABLE III. Relative branching ratios for the decay of resonance series I in terms of absolute cross sections (10^{-17} cm^2). The estimated error for the cross sections is in the order of 20%.

	Exit channel	$v'=0$	$v'=1$	$v'=2$	$v'=3$	$v'=4$	$v'=5$
$B\,^1\Sigma_u^+$	$v=2$	···	0.27	0.39	0.09	0.14	0.14
	$v=1$	···	0.41	0.29	0.39	0.18	0.10
	$v=0$	0.67	1.4	0.76	0.21	···	···
$b\,^3\Sigma_u^{+\,a}$	11.02 eV	···	0.11	0.10	0.042	0.020	0.008
	10.76 eV	0.031	0.087	0.063	0.039	0.015	···
	10.47 eV	0.042	0.063	0.048	0.024	0.007	···
	10.17 eV	0.033	0.045	0.022	0.011	0.004	···
$b\,^3\Sigma_u^+$	Integrated values	2.0	2.5	2.5	1.4	1.0	
$X\,^1\Sigma_g^+$	$v=5$	···	0.09	···	···	···	···
	$v=4$	0.04	0.2	0.06	0.02	···	···
	$v=3$	0.14	0.23	0.02	···	···	···
	$v=2$						
	$v=1$	Pronounced interference structure, see text.					
	$v=0$						

[a] Within an energy band of $\Delta E \approx 60$ meV.

between resonant and nonresonant scattering occurs. Therefore, it seems to be necessary to carry out a complete partial-wave analysis for the e-H_2 scattering problem for elastic and inelastic scattering in order to get a complete set of branching ratios. Such an analysis is outside the framework of this investigation, and instead, a simplified model was used for an estimation of resonance contributions in the $X\ ^1\Sigma_g^+$ ($v=0, 1, 2$) channels.

In Table III relative branching ratios in terms of absolute total cross sections have been listed for those channels where practically no direct-scattering amplitude is present, i.e., for the $v=0$, 1, 2 vibrational channels of the $B\ ^1\Sigma_u^+$ state and for the $v=3$, 4, 5 channels of the $X\ ^1\Sigma_g^+$ state (ground state). In the excitation functions of the $b\ ^3\Sigma_u^+$ continuum state the resonances appear as peaks superimposed on a nonresonant-scattering contribution of approximately equal magnitude (see Fig. 4). In Table III the absolute intensities of these peaks (nonresonant contribution subtracted) have been listed. The uncertainty of these values (approximately 30%) is somewhat higher than in the other cases because of experimental difficulties in measuring the excitation of a continuum state.

One has to be cautious when comparing the values for the $b\ ^3\Sigma_u^+$ state directly with the other values in the table in terms of branching ratios or partial widths, since the resonance peaks may be enhanced by the interference term of the resonant and direct-scattering amplitude. In the table only the measured intensities of the resonance peaks have been considered. The decay probabilities show a clear dependence on the positions of the energy windows in the $b\ ^3\Sigma_u^+$ continuum state. The nearer the winow of the continuum state lies to the decaying resonance state, the higher the decay probability is into this energy window. Integrated cross sections (over all accessible energy windows) are also given in the table. These values represent the total cross sections for resonance scattering into the electronic $b\ ^3\Sigma_u^+$ state.

The decay of the resonance into the electronic ground state is practically free from direct-scattering contributions only in the vibrational channels $v=3$, 4, 5, whereas, in the channels $v=0$, 1, 2, strong interference with the nonresonant scattering amplitude occurs. Therefore, for the latter channels the extraction of quantitative cross sections for the resonance process from the measured data is not possible without carefully analyzing the interference structure. However, one can gain information by using the following model which is valid, at least, for a spherically symmetrical system (see, for example, Ref. 24). This model describes the occurrence of a resonance by letting the scattering amplitude trace out a circle in the complex plane with a certain radius R, which is determined from the minimum and maximum intensities of the resonance line. The value $4R^2$ can then be taken as a measure for the pure resonance effect in this channel. For example, in the case of elastic scattering (channel $v=0$) the resonance effect is very large in absolute units. However, the model shows that this is not due to a large resonant scattering amplitude, but arises from the coherent superposition of a quite small resonant amplitude on a very large direct-scattering amplitude. The applicability of this simple model to molecules needs careful study, but the model seems reasonable inasmuch as we find that it gives values for the channels $v=0$, 1, 2 which are of the same order of magnitude as have been measured for the channels $v=3$, 4, 5. The measurements of the excitation functions for the channels $v=0$, 1, 2 have been presented in absolute units (Figs. 5–7). In this form, besides being of practical interest, the curves contain the material needed for the determination of quantitative branching ratios when a detailed theory becomes available.

Summarizing the results of Table III, one can state that the probability for the decay of resonance series I into the three electronic states $X\ ^1\Sigma_g^+$, $b\ ^3\Sigma_u^+$, and $B\ ^1\Sigma_u^+$ of the H_2 molecule summed over all vibrational states of the exit channel are of the same order of magnitude. This behavior of resonance series I is contrary to the behavior of the other two resonance series discussed in this paper.

ACKNOWLEDGMENTS

We wish to acknowledge gratefully the financial support of the Deutsche Forschungsgemeinschaft. One of us (A.W.) would like to express appreciation to St. Francis Xavier University for a leave of absence and financial support, to Dr. E. M. Clarke for encouragement and advice, to the National Research Council of Canada for a travel grant, and to the Nerken Fund for a special supplementary grant.

---

*On leave of absence (1968/69) from the Physics Department, Saint Francis Xavier University, Antigonish, Nova Scotia, Canada.

[1] H. S. Taylor and J. K. Williams, J. Chem. Phys. 42, 4063 (1965).

[2] I. Eliezer, H. S. Taylor, and J. K. Williams, J. Chem. Phys. 47, 2165 (1967).

[3] C. K. Kuyatt, J. A. Simpson, and S. R. Mielczarek,

J. Chem. Phys. 44, 437 (1966).

[4] G. J. Schulz and R. K. Asundi, Phys. Rev. 158, 25 (1967).

[5] H. Ehrhardt, L. Langhans, F. Linder, and H. S. Taylor, Phys. Rev. 173, 222 (1968).

[6] J. N. Bardsley and F. Mandl, Rept. Progr. Phys. 31, 471 (1968).

[7] H. Ehrhardt and A. Weingartshofer, Z. Physik 226, 28 (1969).

[8] D. E. Golden and H. W. Bandel, Phys. Rev. Letters 14, 1010 (1965).

[9] H. G. M. Heideman, C. E. Kuyatt, and G. E. Chamberlain, J. Chem. Phys. 44, 440 (1966).

[10] M. G. Menendez and Helen K. Holt, J. Chem. Phys. 45, 2743 (1966).

[11] H. Ehrhardt, L. Langhans, and F. Linder, Z. Physik 214, 179 (1968).

[12] C. Ramsauer and R. Kollath, Ann. Physik 12, 529 (1932).

[13] D. E. Golden, H. W. Bandel, and I. A. Salerno, Phys. Rev. 146, 40 (1966).

[14] F. H. Read, J. Phys. B1, 893 (1968).

[15] J. N. Bardsley and F. H. Read, Chem. Phys. Letters 2, 333 (1968).

[16] T. O'Malley and H. S. Taylor, Phys. Rev. 176, 207 (1968).

[17] J. William McGowan and J. F. Williams, *Abstracts of Papers, Sixth International Conference on the Physics of Electronic and Atomic Collisions, Cambridge, Mass.*, 1969 (The MIT Press, Cambridge, Mass., 1969), p. 506.

[18] S. Trajmar, D. C. Cartright, J. K. Rice, R. T. Brinkmann, and A. Kuppermann, J. Chem. Phys. 49, 5464 (1968).

[19] J. Comer and F. H. Read, in Ref. 17, p. 87.

[20] S. Trajmar, D. G. Truhlar, J. K. Rice, and A. Kuppermann, J. Chem. Phys. (to be published).

[21] J. T. Dowell and T. E. Sharp, J. Chem. Phys. 47, 5068 (1967).

[22] R. I. Hall, A. Dumas, J. Mazeau, and J. Reinhardt, in Ref. 17, p. 95.

[23] J. M. Blatt and V. F. Weisskopf, *Theoretical Nuclear Physics* (Wiley, New York, 1952).

[24] D. Andrick, H. Ehrhardt, and M. Eyb, Z. Physik 214, 388 (1968).

PHYSICAL REVIEW A VOLUME 2, NUMBER 2 AUGUST 1970

Phase-Amplitude Method in Atomic Physics. I. Basic Formulas for an Electron in an Ionic Potential*

J. L. Dehmer†
Departments of Chemistry and Physics, University of Chicago, Chicago, Illinois 60637
and
U. Fano
Department of Physics, University of Chicago, Chicago, Illinois 60637

(Received 27 February 1970)

The radial Schrödinger equation for a modified Coulomb field is separated into two first-order equations for a "phase" function and an "amplitude" function which vary only in the non-Coulomb region $r<r_0$. At $r=r_0$, these functions are related to the mixing parameter and normalization constant of quantum-defect theory. Integrals over the range $[0, r_0]$ give the scattering phase shift and the wave function's amplitude near the nucleus. Phase shifts for negative energies serve to calculate the discrete eigenvalues of an atom or positive ion. A numerical procedure for this approach is outlined.

I. INTRODUCTION

This paper originates from an attempt to explain the behavior of inner-shell photoabsorption cross sections. Since these cross sections are proportional[1] to the square of the final state's amplitude near the nucleus, their interpretation requires a suitable formulation of this amplitude in terms of the factors that influence it. The phase-amplitude method[2] (PAM) serves this purpose by representing the inner amplitude in terms of a definite integral over the non-Coulomb part of the potential, provided one utilizes as basis functions a pair of solutions of the Coulomb-field wave equation. The same method also produces a finite-range integral expression for the exact scattering phase shift.

In the last decade, Calogero and others[3] have developed this method in the context of potential scattering. However, this recent progress has treated explicitly only potentials which vanish faster than r^{-1} and has not yet applied the PAM to the broader range of problems for which it is useful.

This paper further develops the PAM in three ways: (a) It derives basic PAM formulas for the case of a modified Coulomb field. (b) It describes